1994ApJ...433..886W

THE ASTROPHYSICAL JOURNAL, 433:886–894, 1994 October 1
© 1994. The American Astronomical Society. All rights reserved. Printed in U.S.A.

PRE- AND POSTPERIHELION ABUNDANCES OF GAS AND DUST IN COMET HALLEY

MARIA WOMACK[1] AND BARRY L. LUTZ
Department of Physics and Astronomy, Box 6010, Northern Arizona University, Flagstaff, AZ 86011
AND
R. MARK WAGNER
Department of Astronomy, Ohio State University, Columbus, OH 43210
Received 1993 June 1; accepted 1994 April 4

ABSTRACT

Photometrically calibrated spectra of comet P/Halley (1986 III) were recorded between 1985 September 12–1986 June 10 using the Ohio State University Image Dissector Scanner on the Perkins 72 inch telescope at the Lowell Observatory. Column densities of CN, C_3, CH, C_2, and NH_2 were calculated from measured fluxes in these spectra, and molecular scale lengths were deduced from the radial distribution of CN, C_3, C_2, and NH_2. Production rates were computed using the new scale lengths and a Haser model analysis. Continuum emission at 4260 Å was used to derive gas-to-dust ratios. The data indicate than comet Halley was ~2–5 times more abundant in gas and dust at postperihelion than preperihelion. On 1986 June 8 we observed the onset of a cometary outburst which appeared very strong in dust production. The gas-to-dust ratios appeared to be subject to changes as a result of short-term outbursts but otherwise did not exhibit any systematic dependence on heliocentric distance. Reflectivity gradients of the continuum were also measured from the spectra. While most of the continua were red, blue continua were also observed which may be correlated with dust outbursts.

Subject headings: comets: individual (Halley) — molecular processes

1. INTRODUCTION

The reappearance of comet Halley in 1985–1986 provided an excellent opportunity to observe a comet's behavior as it traveled past the Sun. The production of dust and gas in many comets has been observed to vary significantly between the inbound and outbound parts of their passage by the Sun (e.g., Weissman 1987; Houpis 1989; Cochran et al. 1992). Furthermore, cometary production rates often vary by up to factors of 2 on a daily basis (e.g., Schleicher et al. 1990). Outbursts have been also observed in comae (Lutz & Wagner 1986; Meech & Jewitt 1987; Rozenbush et al. 1989). Unfortunately, only a few comets have been studied in detail with a good coverage of heliocentric distances. The long predicted appearance of comet Halley in 1985/86 afforded the opportunity to temporally map its evolution over an extended arc of its orbit centered on perihelion.

We obtained optical spectra of comet Halley during the period of 1985 September–1986 June covering the heliocentric distances of $r = -2.64$ to $+2.09$ AU. The ionized species N_2^+, CO^+, and H_2O^+ observed in these spectra have been discussed elsewhere (Lutz, Womack, & Wagner 1993). In this paper we present the measured fluxes and column densities of the dominant neutral species and the derived production rates. We also discuss relative molecular abundances and differences in cometary volatiles and dust production preperihelion versus postperihelion.

2. OBSERVATIONS AND RESULTS

Spectra of comet Halley were obtained over the period of 1985 September 12–1986 June 10 using the Ohio State University Image Dissector Scanner (Byard et al. 1981) on the Perkins 72 inch telescope of the Ohio State University at the Lowell Observatory (see Table 1). The dual beam circular entrance apertures of the spectrograph corresponded to 6.″4 in diameter on the plane of the sky and were separated by 39″ center to center. The projected spatial extent of the aperture diameters is given for each date in Table 1. A 600 lines mm^{-1} grating blazed at 5500 Å was employed covering the wavelength region 3750–6350 Å with a spectral resolution of ~10 Å. The wavelengths were calibrated using FeNeHe lamp frames, and the spectra were flux-calibrated using a sensitivity function obtained from the standard stars EG 29, HZ 15, EG 139, EG 248, EG 42, and Feige 110. A list of the molecular features observed in this region is provided in Table 2. The position angle (P.A.) (measured north through east) and projected offset of the spectrograph slit from the comet on the plane of the sky is given in Table 3 for each spectrum. A negative value of the offset refers to the sunward direction.

Removal of sky features was performed by subtracting spectra of the night sky obtained 2.°5 from the comet from each comet spectrum. A solar analog star, van Bueren 64 (Hardorp 1982), was observed on 1985 September 12 with the same instrumental configuration as for the comet and was used to remove the reflected solar continuum from all of the cometary spectra. Continuum bandpasses were chosen based on observations of other comets (e.g., Wagner, Lutz, & Wyckoff 1987), and continuum fluxes were measured in both the comet and solar analog spectra. The spectrum of the solar analog star was then scaled to the cometary continuum fluxes and subtracted from the observed comet spectrum to produce the spectrum of the gaseous emission in its coma. Table 3 gives integrated fluxes of molecules and continuum bandpasses from all of the spectra. The reduced data (without subtraction of the solar continuum) are included in the International Halley Watch CD-ROM Archive (Wagner & Lutz 1992).

A spectrum obtained of the nuclear region of Halley (with the solar continuum subtracted) on 1986 January 10 is shown in Figure 1. Denoted in the figure are transitions of CN, C_3, CH, C_2, and NH_2 and the selected continuum bandpass. A

[1] Currently at Division of Science, Pennsylvania State University, Erie, PA 16563.

© American Astronomical Society • Provided by the NASA Astrophysics Data System

1994ApJ...433..886W

TABLE 1

OBSERVATIONS OF COMET HALLEY

Date	r (AU)	Δ (AU)	Aperture (km)
19850912.....	2.59	2.64	12254
19850914.....	2.56	2.58	11976
19850915.....	2.55	2.55	11836
19851211.....	1.33	0.75	3481
19851213.....	1.30	0.79	3667
19851214.....	1.28	0.80	3714
19860110.....	0.87	1.32	6127
19860112.....	0.84	1.34	6220
19860513.....	1.81	1.18	5477
19860514.....	1.82	1.21	5616
19860608.....	2.17	2.03	9423
19860610.....	2.20	2.09	9701

possible cometary outburst in dust was observed in the spectrum of 1986 June 8, which is shown in Figure 2, without subtraction of the solar spectrum. For comparison, the 1986 June 10 spectrum (without subtraction of the solar spectrum) is shown in Figure 2 to demonstrate the appreciably different relative dust production on these two days.

3. DISCUSSION

3.1. *Column Densities and Production Rates*

Electronic transitions of cometary molecules are excited by resonance fluorescence, so that the column density, N, of a molecule along the line of sight to the comet is given by

$$N = \frac{4\pi F}{\Omega g}, \quad (1)$$

where F is the integrated molecular band flux, Ω is the solid angle subtended by the spectrographs slit at the comet, and g is the fluorescence efficiency, or g-factor, of the molecule.

TABLE 2

OBSERVED FEATURES IN COMET HALLEY

Molecule	Transition	Wavelength (Å)	Fluorescence Efficiency (molecules s^{-1})
CN	$B\,^2\Sigma^+ - X\,^2\Sigma$ ($\Delta v = 0$)	3883	...[a]
C_3	$^1\Pi_u - {}^1\Sigma_g^+$ ($\Delta v = 0$)	4050	0.2037[b]
CN	$B\,^2\Sigma^+ - X\,^2\Sigma^+$ ($\Delta v = -1$)	4216	0.0047[c]
CH	$A\,^2\Delta - X\,^1\Sigma^+$ ($\Delta v = 0$)	4314	0.0220[d]
C_2	$d\,^3\Pi_g - a\,^3\Pi_u$ ($\Delta v = +1$)	4737	0.0530[e]
C_2	$d\,^3\Pi_g - a\,^3\Pi_u$ ($\Delta v = +0$)	5165	0.1160[e]
C_2	$d\,^3\Pi_g - a\,^3\Pi_u$ ($\Delta v = -1$)	5635	0.0690[e]
NH_2	$^2A_1\,\Pi_u - {}^2B_1\,\Sigma_g$ (10–0) Π	5730	0.0053[f]
NH_2	$^2A_1\,\Pi_u - {}^2B_1\,\Sigma_g$ (9–0) Σ, Δ	5982, 6060	0.0060[f]
Continuum	...	4240–4280	...

[a] Dependent on heliocentric velocity; Schleicher 1981.
[b] A'Hearn 1982.
[c] Schleicher 1981.
[d] Lutz, Womack, & Wagner 1993.
[e] Wyckoff et al. 1988.
[f] Tegler & Wyckoff 1989.

Fluorescence efficiencies for the molecules of interest at 1 AU are listed in Table 2 and were scaled to the appropriate heliocentric distance, r(AU), according to $g(r) = g(1\ \mathrm{AU})/r^2$. For the CN (0–0) band, the Swings effect on the molecular excitation has been taken into account, and the corresponding g-factor for the heliocentric velocity of the comet for each night was taken from Schleicher (1981).

Column densities of CN, C_3, CH, C_2, and NH_2 were calculated for comet Halley and are presented in Table 4. More than one transition was observed for CN, C_2, and NH_2. Since molecular column densities should be identical regardless of which transition is used for the calculation, column densities were determined for all bands to derive an average result for the molecule whenever possible. Within the uncertainties, good

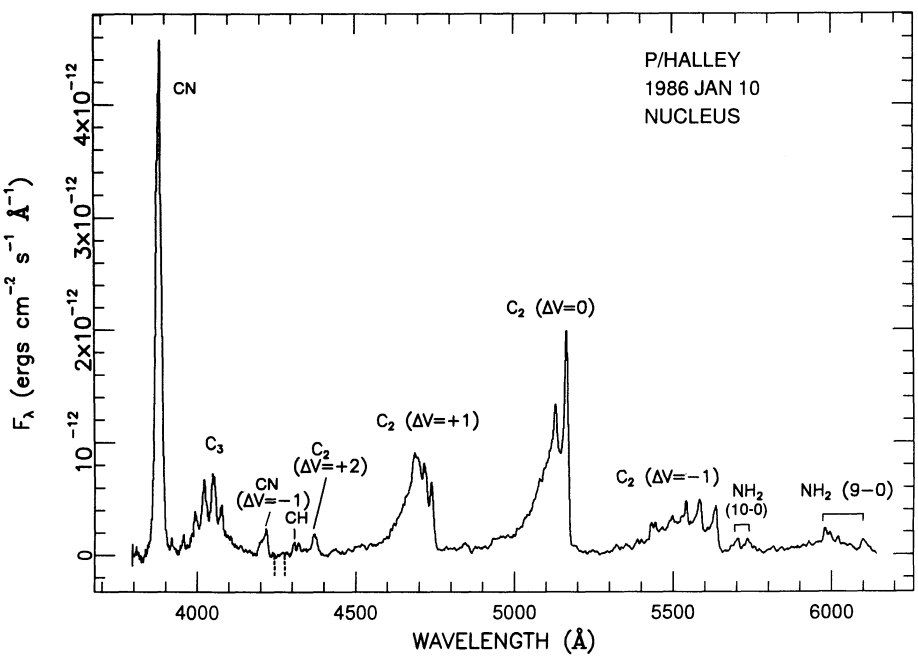

FIG. 1.—Spectrum of the nuclear region of comet Halley obtained on 1986 January 10. Positions of molecular species are denoted. The continuum bandpass at ~4260 Å which was used in the analysis is denoted by vertical dashed lines.

© American Astronomical Society • Provided by the NASA Astrophysics Data System

1994ApJ...433..886W

TABLE 3

OBSERVED FLUXES IN COMET HALLEY

UT DATE	OFFSET[a] (km)	P.A.	F_λ (10^{-13} ergs cm^{-2} s^{-1}) CN (0–0)	C_3	CN (0–1)	CH	C_2 (2–0)	C_2 (1–0)	C_2 (0–0)	C_2 (0–1)	NH_2 (10–0)	NH_2 (9–0)	Continuum
19850912.....	0	0	1.0 ± 0.2	...	...	...	...	...	...	...	...	...	1.2 ± 0.2
19850914.....	0	0	1.6 ± 0.4	...	...	...	...	...	...	...	...	...	1.3 ± 0.3
19850915.....	0	0	0.6 ± 0.1	...	...	...	...	...	...	...	...	...	0.6 ± 0.1
19851211.....	0	0	33.8 ± 6.8	28.0 ± 5.6	3.6 ± 0.7	1.0 ± 0.3	...	28.1 ± 5.6	66 ± 13	27.6 ± 5.5	5.4 ± 1.1	10.0 ± 7.0	6.3 ± 1.3
19851211.....	−10879	270	27.0 ± 5.4	15.0 ± 3.2	1.9 ± 0.4	...	...	17.0 ± 3.4	38.0 ± 7.4	15.0 ± 3.2	1.3 ± 0.3	3.0 ± 0.6	1.8 ± 0.4
19851211.....	−21758	270	78.0 ± 15.4	19.0 ± 3.7	4.3 ± 0.8	0.8 ± 0.2	1.6 ± 0.3	38.0 ± 7.4	80 ± 17	33.0 ± 6.4	1.8 ± 0.3	3.7 ± 0.8	3.1 ± 0.5
19851211.....	−163183	250	0.9 ± 0.2	...	...	...	...	0.5 ± 0.1	1.3 ± 0.3	0.7 ± 0.1	...	...	...
19851211.....	10879	90	22.0 ± 4.5	10.0 ± 2.0	1.4 ± 0.3	...	0.5 ± 0.1	15.0 ± 0.3	32.0 ± 6.4	13.0 ± 0.2	1.0 ± 0.2	2.6 ± 0.5	1.4 ± 0.3
19851211.....	65546*	70	23.9 ± 4.8	5.0 ± 1.0	1.3 ± 0.3	...	0.7 ± 0.1	14.0 ± 2.8	29.0 ± 5.8	11.0 ± 2.2	0.6 ± 0.1	1.4 ± 0.4	0.9 ± 0.2
19851213.....	−10313	270	68.0 ± 13.6	25 ± 5	3.5 ± 0.7	0.7 ± 0.2	1.7 ± 0.4	46.0 ± 9.2	100 ± 20	48 ± 9.6	4.3 ± 0.9	11.0 ± 2.2	4.1 ± 0.8
19851213.....	−12605*	180	67.0 ± 13.4	25.0 ± 5.0	3.2 ± 0.6	0.6 ± 0.2	1.8 ± 0.4	45 ± 9	96.0 ± 19.2	45.0 ± 9.0	3.5 ± 0.7	9.9 ± 3.0	4.1 ± 0.8
19851213.....	−17189*	180	49.0 ± 9.8	16.0 ± 3.2	2.8 ± 0.6	0.4 ± 0.1	1.2 ± 0.2	36.0 ± 7.2	70 ± 14	34.0 ± 6.8	2.3 ± 0.5	6.6 ± 2.0	2.6 ± 0.5
19851213.....	10313	90	82.0 ± 16.4	40 ± 8	4.3 ± 0.9	1.0 ± 0.2	1.9 ± 0.4	54 ± 11	110 ± 22	48.0 ± 9.6	4.4 ± 0.9	13.0 ± 2.6	4.2 ± 0.8
19851213.....	12605*	0	76.0 ± 15.2	27.0 ± 5.4	3.4 ± 0.7	1.0 ± 0.2	1.6 ± 0.3	49.0 ± 9.8	100 ± 20	47.0 ± 9.4	3.5 ± 0.7	9.1 ± 2.7	3.5 ± 0.7
19851213.....	17189*	0	51.0 ± 10.2	19.0 ± 3.8	2.5 ± 0.5	...	1.1 ± 0.2	32.0 ± 6.4	69.0 ± 13.8	30.0 ± 6.0	1.8 ± 0.4	5.0 ± 1.5	1.7 ± 0.3
19851213.....	22918*	0	47.0 ± 9.6	8.0 ± 1.6	1.6 ± 0.3	...	...	23.0 ± 5.0	47.0 ± 0.9	22.0 ± 4.3	1.1 ± 0.2	3.2 ± 0.6	1.0 ± 0.2
19851213.....	171889*	70	8.9 ± 1.2	...	0.24 ± 0.05	...	...	3.9 ± 0.8	7.2 ± 1.4	3.5 ± 0.7	...	...	0.20 ± 0.04
19851213.....	343775*	70	2.6 ± 0.5	...	...	...	...	0.7 ± 0.2	1.4 ± 0.3	0.7 ± 0.1	...	...	...
19851214.....	0	0	74 ± 15	60 ± 12	4.5 ± 0.9	...	3.2 ± 0.6	64 ± 13	110 ± 22	66.0 ± 13.2	7.8 ± 1.6	15.0 ± 4.5	14.0 ± 2.8
19851214.....	−8703	249	55 ± 11	26.0 ± 5.2	2.7 ± 0.5	...	...	40.0 ± 8.0	71.0 ± 14.2	37.0 ± 7.4	3.5 ± 0.7	7.8 ± 2.3	4.5 ± 0.9
19851214.....	−20307*	260	37.0 ± 7.4	11.0 ± 2.2	1.8 ± 0.4	...	1.1 ± 0.2	30.0 ± 6.0	56.0 ± 11.2	27.0 ± 5.4	1.7 ± 0.3	3.6 ± 1.1	1.7 ± 0.3
19851214.....	−31331	264	34.0 ± 6.8	7.4 ± 1.5	2.3 ± 0.5	...	1.7 ± 0.3	27.0 ± 5.4	48.0 ± 9.6	23.0 ± 4.6	1.2 ± 0.2	3.3 ± 1.0	1.1 ± 0.2
19851214.....	−37714*	255	27.0 ± 5.4	6.4 ± 1.3	1.8 ± 0.4	0.5 ± 0.1	1.0 ± 0.2	19.0 ± 3.8	35.0 ± 7.0	16.0 ± 3.2	0.7 ± 0.1	1.6 ± 0.5	0.4 ± 0.1
19851214.....	−56860	257	18.0 ± 3.6	2.7 ± 0.5	1.1 ± 0.2	...	0.9 ± 0.2	14.0 ± 2.8	24.0 ± 4.8	11.0 ± 2.2	...	...	...
19851214.....	−69625	249	16.0 ± 3.2	1.3 ± 0.3	0.8 ± 0.2	...	0.9 ± 0.2	14.0 ± 1.9	17.0 ± 3.4	7.7 ± 1.5	0.3 ± 0.1	1.0 ± 0.3	...
19851214.....	−91673	254	11.0 ± 3.6	2.7 ± 0.2	0.8 ± 0.2	...	0.3 ± 0.1	7.3 ± 1.5	13.0 ± 2.6	5.8 ± 1.2	...	...	...
19851214.....	−139250	249	4.5 ± 0.9	...	...	...	...	2.3 ± 0.5	4.4 ± 0.9	1.9 ± 0.4	...	...	0.04 ± 0.01
19851214.....	−160718	252	5.1 ± 1.0	...	3.3 ± 0.1	...	...	2.7 ± 0.5	4.2 ± 0.8	2.0 ± 0.4	...	...	...
19851214.....	−289525	249	1.3 ± 0.3	...	...	...	...	0.4 ± 0.1	0.9 ± 0.2	0.5 ± 0.1	...	...	...
19851214.....	−393863	249	0.6 ± 0.1	...	...	...	...	0.3 ± 0.1	0.7 ± 0.2	0.5 ± 0.1	...	...	...
19851214.....	−463598	249	0.5 ± 0.1	..	...	...	...	0.4 ± 0.1	0.6 ± 0.1	0.3 ± 0.1	...	...	...
19851214.....	−498402	249	0.20 ± 0.04	...	...	...	...	...	0.3 ± 0.1	...	...	...	...
19851214.....	23208	90	46.0 ± 9.2	16.0 ± 3.2	2.5 ± 0.5	0.6 ± 0.2	1.1 ± 0.2	34.0 ± 6.8	63.0 ± 12.6	32.0 ± 6.4	2.2 ± 0.4	4.8 ± 1.4	2.8 ± 0.6
19851214.....	289525	70	4.5 ± 0.9	...	...	...	...	1.5 ± 0.3	2.9 ± 0.6	1.5 ± 0.3	...	...	...
19851214.....	1044402	70	1.0 ± 0.2	...	...	...	...	...	...	...	...	...	...
19860110.....	0	0	990 ± 198	520 ± 104	54 ± 11	23 ± 6	40 ± 8	790 ± 158	1300 ± 260	720 ± 144	53 ± 10	100 ± 30	120 ± 24
19860112.....	0	0	1400 ± 280	390 ± 78	62 ± 12	30 ± 7	54 ± 11	1100 ± 220	2000 ± 400	1200 ± 240	62 ± 12	140 ± 42	99 ± 20
19860513.....	0	0	25 ± 5	25 ± 5	1.0 ± 0.2	...	...	13.0 ± 2.6	33.0 ± 6.6	17.0 ± 3.4	3.7 ± 0.7	3.7 ± 1.1	14.0 ± 2.8
19860513.....	−29953	270	14.0 ± 2.8	6.4 ± 1.3	1.1 ± 0.2	...	0.4 ± 0.1	8.8 ± 1.8	20.0 ± 4.0	10.0 ± 2.0	0.8 ± 0.2	1.3 ± 0.4	1.6 ± 0.3
19860513.....	29953	90	13.0 ± 2.6	5.3 ± 1.1	0.7 ± 0.1	...	0.4 ± 0.1	9.1 ± 1.8	21.0 ± 4.2	11.0 ± 2.2	0.9 ± 0.2	1.5 ± 0.5	1.8 ± 0.4
19860514.....	0	0	13.0 ± 2.6	15.0 ± 3.0	0.4 ± 0.1	...	...	7.8 ± 1.6	12.0 ± 2.4	7.2 ± 1.4	...	...	6.0 ± 1.2
19860514.....	−9653	270	5.9 ± 1.2	3.7 ± 0.7	0.9 ± 0.2	...	...	5.8 ± 1.2	9.3 ± 1.9	4.3 ± 0.9	...	...	1.2 ± 0.2
19860514.....	−21062	270	8.7 ± 1.7	...	...	...	...	3.9 ± 0.8	8.1 ± 1.6	3.8 ± 0.8	...	...	0.5 ± 0.1
19860514.....	−30715	270	16.0 ± 3.2	16.0 ± 3.2	1.0 ± 0.2	...	...	8.9 ± 1.8	14.0 ± 2.8	8.8 ± 1.8	...	...	5.7 ± 1.1
19860514.....	9653	90	6.7 ± 1.3	...	0.5 ± 0.1	...	...	5.4 ± 1.1	8.1 ± 1.6	5.0 ± 1.0	0.5 ± 0.1	...	0.9 ± 0.2
19860514.....	21062	90	5.9 ± 1.2	4.6 ± 0.9	...	...	...	5.2 ± 1.0	9.0 ± 1.8	4.1 ± 0.8	...	...	1.2 ± 0.2
19860514.....	30715	90	6.9 ± 1.4	2.8 ± 0.6	0.4 ± 0.1	...	...	5.0 ± 1.0	8.9 ± 1.8	3.7 ± 0.7	0.4 ± 0.1	1.0 ± 0.3	1.0 ± 0.2
19860608.....	0	0	12.0 ± 2.4	8.3 ± 1.7	...	...	...	3.6 ± 0.7	4.7 ± 0.9	3.4 ± 0.6	...	...	22.0 ± 4.4
19860608.....	−57419	270	5.1 ± 1.0	2.2 ± 0.4	...	...	...	2.5 ± 0.5	4.3 ± 0.9	2.7 ± 0.5	...	...	1.4 ± 0.3
19860608.....	57419	90	3.0 ± 0.6	2.6 ± 0.5	0.3 ± 0.1	...	...	2.0 ± 0.4	4.0 ± 0.8	1.7 ± 0.3	...	...	1.2 ± 0.2
19860610.....	0	0	8.9 ± 1.8	5.7 ± 1.1	...	...	...	4.8 ± 1.0	6.1 ± 1.2	5.1 ± 1.0	...	...	3.1 ± 0.6

NOTE.—Asterisk (*) denotes files which formed by the co-addition of two nearby frames to increase the signal-to-noise ratio of the spectrum.

[a] A negative value refers to the sunward direction.

© American Astronomical Society • Provided by the NASA Astrophysics Data System

1994ApJ...433..886W

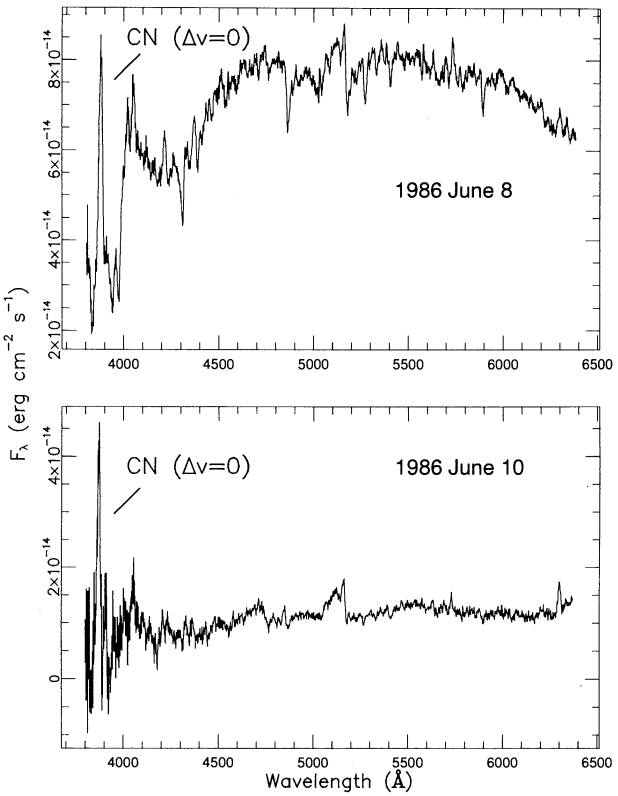

FIG. 2—Spectra of the nuclear region of Halley obtained on (*a*) 1986 June 8, and (*b*) 1986 June 10. The reflected solar continuum appeared ~7 times stronger on June 8 than June 10, while the CN production remained relatively constant during this time period.

agreement was found for column densities of CN derived from the $\Delta v = 0$ and $\Delta v = -1$ bands, and for C_2 using the three most prominent Swan features. In the case of the two transitions of NH_2 which were usually present in the spectra [(10–0) and (9–0)], the (9–0) transition was often contaminated by the underlying C_2 $\Delta v = -2$ transition. Consequently, NH_2 column densities were determined from the (10–0) transition alone.

Production rates were derived from observed column densities using a model which is based on a two-step photodissociation decay process (Haser 1957). While this simple model is not physically realistic, it is often useful for comparing observations of cometary molecules. The model utilizes molecular "scale lengths" (β^{-1}) to characterize a species' creation and destruction in comae. Many different scale lengths typically are found in the literature for an individual molecule, and it is not clear which is the most representative of a molecule's chemistry in a cometary atmosphere (see Table 5). Where necessary, we have converted lifetimes published in the literature to scale lengths by using the relationship $\tau v = \beta^{-1}$, where $v = 1$ km s^{-1}.

In order to better determine molecular scale lengths for our observations, we have constructed spatial profiles of CN, C_3, C_2, and NH_2 from data obtained on Halley on 1985 December 14. These spatial distributions are shown in Figure 3 along with a best-fit of the Haser model using the derived scale lengths in Table 5. We assume a nominal outflow velocity of $v = 1$ km s^{-1} for the parent and daughter molecules. The scale lengths for C_3 and NH_2 are presented in Table 5 as the derived values and should be used with caution, since they were determined from data only within 100,000 km of the nuclear region, which may not cover enough distance to accurately determine the scale lengths. We note, however, that our scale lengths are similar to values determined by other observers. Much more spatial coverage was available for the C_2 and CN emission, and scale lengths for these molecules were determined from data covering two orders of magnitude, ranging from 8700 km to 500,000 km from the nucleus. Our C_2 and CN scale lengths are in good agreement with other published values (see Table 5). Emission from CH was observed at only two positions in the coma on 1985 December 14. Consequently, scale lengths for CH could not be determined from our data. For CH we assumed $\beta_p^{-1} = 90{,}000$ km and $\beta_d^{-1} = 100$ km (Allen et al. 1989). Production rates were derived for CN, C_3, CH, C_2, and NH_2 and are presented in Table 6.

For dust production, we have followed the $Af\rho$ formalism suggested by A'Hearn et al. (1984), where

$$Af\rho = \frac{(2r\Delta)^2 F_{\rm com}}{(\rho F_{\rm sun})}, \qquad (2)$$

is proportional to the production rate, A is the dust grain albedo, f is the filling factor of grains in an aperture of radius ρ (cm), r is the heliocentric distance of the comet (AU), Δ is the geocentric distance (cm), $F_{\rm com}$ is the cometary flux observed at the earth, and $F_{\rm sun}$ is the solar flux at 1 AU, for the same bandpass. The solar flux, $F_{\rm sun} = 6745$ ergs cm^{-1} s^{-2}, inte-

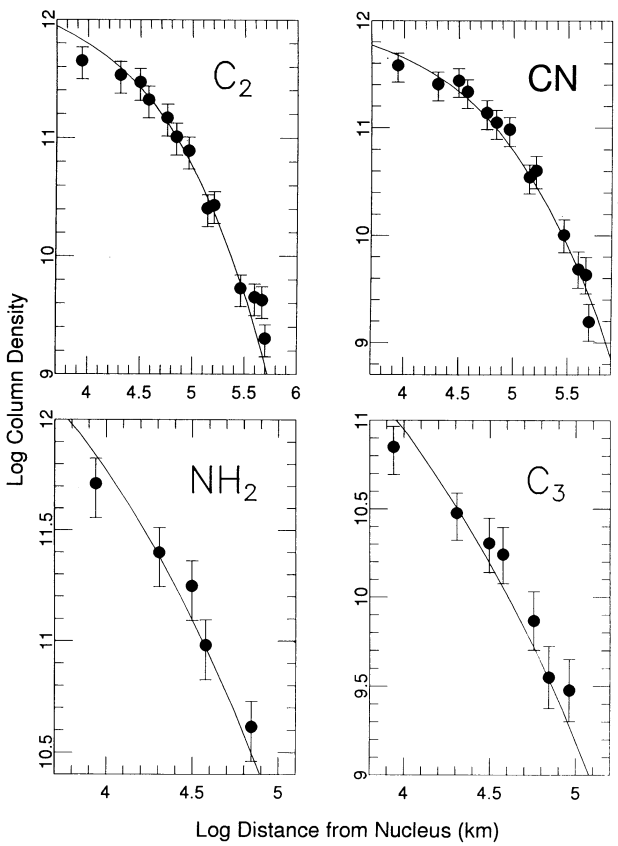

FIG. 3.—Log of measured column densities on 1985 December 14 are plotted in filled circles as a function of radial distance from the nucleus. Solid lines represent a Haser model fitted to the data using the derived scale lengths listed in Table 5.

© American Astronomical Society • Provided by the NASA Astrophysics Data System

1994ApJ...433..886W

TABLE 4

OBSERVED COLUMN DENSITIES

UT DATE	OFFSET (km)	$N(10^{10}$ molecules $cm^{-2})$ CN	C_3	CH	C_2	NH_2
19850912.....	0	2.9 ± 0.9	...	...	...	...
19850914.....	0	4.6 ± 1.4	...	...	...	...
19850915.....	0	1.7 ± 0.5	...	...	...	...
19851211.....	0	38 ± 11	22 ± 6.5	2.9 ± 1.2	38 ± 11	86 ± 26
19851211.....	−10879	19.3 ± 58	12 ± 3.5	...	22 ± 7	21 ± 7
19851211.....	−21758	49 ± 15	15 ± 4.4	2.3 ± 0.3	48 ± 14	29 ± 9
19851211.....	−163183	0.7 ± 0.2	...	...	0.8 ± 0.2	...
19851211.....	10879	14.9 ± 4.5	7.8 ± 2.3	...	19 ± 6	16 ± 5
19851211.....	65546*	19.6 ± 6	1.5 ± 0.4	...	17 ± 5.1	8.9 ± 2.7
19851213.....	−10313	39 ± 12	18 ± 5.4	2.0 ± 0.6	59 ± 18	72 ± 14
19851213.....	−12605*	47 ± 14	7.0 ± 2.1	1.7 ± 0.7	57 ± 17	53 ± 16
19851213.....	−17198*	37 ± 11	4.5 ± 1.3	1.2 ± 0.5	43 ± 13	35 ± 11
19851213.....	10313	48 ± 14	30 ± 9	2.8 ± 0.8	64 ± 19	70 ± 14
19851213.....	12605*	52 ± 16	7.6 ± 2.3	2.7 ± 1.1	60 ± 18	53 ± 16
19851213.....	17189*	36 ± 11	5.3 ± 1.6	...	40 ± 12	27 ± 8.2
19851213.....	22918*	23 ± 6.8	5.9 ± 1.8	...	28 ± 8	18 ± 5
19851213.....	171889*	5.1 ± 1.5	...	...	4.5 ± 1.4	...
19851213.....	343775*	2.1 ± 0.6	...	...	0.9 ± 0.3	...
19851214.....	0	56 ± 17	16 ± 5	...	74 ± 22	115 ± 34
19851214.....	−8703	38.0 ± 11.4	7.1 ± 2.1	...	45 ± 13	52 ± 16
19851214.....	−20307*	26 ± 8	3.0 ± 0.9	...	34 ± 10.2	25.0 ± 7.5
19851214.....	−31331	27.3 ± 8.2	2.0 ± 0.6	...	30 ± 9	17.7 ± 5.3
19851214.....	−37714*	21.6 ± 6.5	1.7 ± 0.5	1.4 ± 0.6	21 ± 6.3	9.6 ± 2.9
19851214.....	−56860	13.8 ± 4.1	0.7 ± 0.2	...	14.8 ± 4.4	...
19851214.....	−69625	11.2 ± 3.4	...	...	10.2 ± 3.1	4.1 ± 1.2
19851214.....	−91673	9.6 ± 2.9	0.3 ± 0.1	0.4 ± 0.2	7.8 ± 2.3	...
19851214.....	−139250	3.5 ± 1.1	...	...	2.6 ± 0.8	...
19851214.....	−160718	4.1 ± 1.2	...	...	2.7 ± 0.8	...
19851214.....	−289525	1.0 ± 0.3	...	...	0.5 ± 0.2	...
19851214.....	−393963	0.5 ± 0.1	...	...	0.5 ± 0.1	...
19851214.....	−463598	0.4 ± 0.1	...	...	0.4 ± 0.1	...
19851214.....	−498402	0.16 ± 0.05	...	...	0.20 ± 0.06	...
19851214.....	23208	33 ± 10	4.4 ± 1.3	1.5 ± 0.6	39 ± 12	32 ± 9.7
19851214.....	289525	3.5 ± 1.1	...	...	1.8 ± 0.5	...
19851214.....	1044402	0.8 ± 0.2	...	...	...	...
19850110.....	0	331 ± 99	65 ± 20	29 ± 11	400 ± 119	360 ± 108
19850112.....	0	399 ± 120	46 ± 14	35 ± 14	564 ± 169	393 ± 118
19850513.....	0	34 ± 10	14 ± 4	...	37 ± 11	109 ± 33
19850513.....	−29953	25.4 ± 7.6	3.5 ± 1.0	...	22.9 ± 6.9	23.5 ± 7.1
19850513.....	29953	19.4 ± 5.8	2.9 ± 0.9	...	24.3 ± 7.3	26.5 ± 7.9
19850514.....	0	15.9 ± 4.8	8.3 ± 2.5	...	16.9 ± 5.1	...
19850514.....	−9653	15.6 ± 4.7	2.0 ± 0.6	...	11.9 ± 3.6	...
19850514.....	−21062	15.0 ± 4.5	...	...	9.5 ± 2.8	...
19850514.....	−30715	25.7 ± 7.7	8.8 ± 2.6	...	19.8 ± 5.9	...
19850514.....	9653	12.2 ± 3.7	...	...	11.6 ± 3.5	15.8 ± 4.7
19850514.....	21062	10.2 ± 3.0	2.5 ± 0.8	...	11.1 ± 3.3	...
19850514.....	30715	11.3 ± 3.4	1.5 ± 0.5	...	10.6 ± 3.2	12.8 ± 3.8
19850608.....	0	29.3 ± 8.8	6.4 ± 2.1	...	10.4 ± 3.2	...
19850608.....	−57419	12.5 ± 3.7	1.7 ± 0.5	...	8.4 ± 2.5	...
19850608.....	57419	8.4 ± 2.5	2.0 ± 0.6	...	6.5 ± 2.0	...
19850610.....	0	22.4 ± 6.7	4.6 ± 1.4	...	15.0 ± 4.5	...

NOTE.—Asterisk (*) denotes files which were co-added from two nearby frames to increase the signal-to-noise ratio of the spectrum.

grated over the bandpass given in Table 2 for 1 AU was obtained from Kurucz et al. (1984). $Af\rho$ values have been calculated for the nuclear position for each date and are listed in Table 6.

3.2. *Gas-to-Dust Ratios*

The relative amounts of volatiles and solid grains in a cometary atmosphere are often measured with the hopes of learning about the physical composition of the nucleus. A homogeneous nucleus is expected to release gas and dust in the same relative amounts throughout its perihelion passage. On the other hand, a nonuniformly mixed nucleus may yield a gas/dust abundance ratio that varies over time. Thus, a gas-to-dust ratio (GDR) is often used as an indicator of how closely the gas is tied to the dust. To derive this quantity, we compared the total gas production to $Af\rho$, which is proportional to the dust production.

Water is the dominant volatile in most comets, and its production rate, which is usually determined from observations of OH and [O I], is assumed to represent the total gas production. Due to its prominence in optical spectra, however, CN emission is often used to determine the total gas production

© American Astronomical Society • Provided by the NASA Astrophysics Data System

1994ApJ...433..886W

TABLE 5

ADOPTED MOLECULAR SCALE LENGTHS

Molecule	β_p^{-1} (km)	β_d^{-1} (km)	Reference
CN	25000	190000	1
CN	15000	190000	2
CN	16000	330000	3
CN	17000	300000	4
C_3	3200	80000	1
C_3	3200	25000	2
C_3	3100	150000	4
C_3	1000	60000	5
CH	90000	100	6, 7
CH	120000	6000	3
CH	85000	108	8
C_2	25000	100000	1
C_2	20000	70000	2
C_2	32000	100000	3
C_2	25000	120000	4
NH_2	4000	50000	1, 9
NH_2	4000	40000	10
NH_2	4100	62000	11
NH_2	3800	79000	12

REFERENCES.—(1) Derived; (2) Randall 1992; (3) Wyckoff et al. 1988; (4) Cochran 1986; (5) A'Hearn 1982; (6) Adopted; (7) Allen et al. 1989; (8) Huebner, Keady, & Lyon 1992; (9) Tegler et al. 1992; (10) Debi Prasad, Jockers, & Geyer 1992; (11) Cochran et al. 1992; (12) Fink, Combi, & Di Santi 1991.

rate, under the assumption that Q(OH)/Q(CN), and hence Q(CN)/Q(H_2O), is approximately constant. Recently, however, a study of CN and OH in many comets over wide ranges of heliocentric distances found that the ratio Q(OH)/Q(CN) can vary by up to a factor of 2 over the course of a few days and that no singular value for the Q(OH)/Q(CN) ratio can be established for an entire cometary orbit (Schleicher et al. 1993). For the most part, however, the Q(OH)/Q(CN) ratios did not change significantly on a day-to-day basis. We therefore utilized a Q(OH)/Q(CN) ratio determined by Schleicher et al. (1993) for the same date as our observation, or within 2 days of our observation, to derive OH production rates from our CN observations. These Q(OH)/Q(CN) ratios are listed in Table 6. Water production rates were calculated using these Q(OH)/Q(CN) ratios, our derived CN production rates, and an assumed photodissociation branching ratio of 93% for H_2O into OH. The derived water production rates were assumed to represent the total gas production rates and are also listed in Table 6.

The measured quantity $Af\rho$ described in § 3.1 was considered to be directly proportional to the cometary dust production rate. GDRs were calculated using GDR = log [$Q(H_2O)/Af\rho$] − 24. The arbitrary scaling factor of 24 has no physical meaning and was used to make the numbers easier to compare with other derived rates in the literature and to look for trends in GDRs over time. The calculated GDRs are listed in Table 6. Assuming an uncertainty of 35% in Q(CN), 20% in Q(OH)/Q(CN), and 25% in $Af\rho$, we estimate the relative GDR calculated here to be accurate to within ∼0.2.

The GDRs do not appear to vary systematically with heliocentric distance. As Table 6 shows, most of the ratios measured for Halley in September, January, May, and June were consistent with the average value of GDR = 1.3 ± 0.2. However, significant deviations are present in the December data, where the ratio was GDR ∼ 2.1, an increase by a factor of ∼10 in the gas production relative to dust production, compared to the September data, when GDR ∼ 1.1. The GDR remained high over the three days in December for which we have data. In January, the production of gas relative to dust decreased by a factor of ∼5, returning to approximately the average value. Another significant variation in gas and dust production occurred in June, when over the course of 2 days, the dust production decreased by a factor of 7 while the gas production remained relatively constant (see Table 6). During this time period, the GDR changed from 0.7 on June 8 to 1.4 on June 10, indicating an overall decrease in the dust production relative to the gas production of a factor of ∼5.

Given the high value for $Af\rho$ of ∼12,000 on June 8 and that the gas production appeared relatively constant between June 8 and 10, it is possible that the low GDR of 0.7 on June 8 indicates that an outburst occurred primarily comprised of dust. As Figure 2 shows, the optical spectrum of comet Halley was dominated by reflected solar continuum, which was significantly lower 2 days later on June 10, while the CN production rate was ∼30% higher on June 8 than June 10. The C_3 production rate was ∼50% higher on June 8 than June 10, while the C_2 production rate was approximately constant over this time period. The increased dust production appears local-

TABLE 6

PRODUCTION RATES IN COMET HALLEY

UT Date	r (AU)	Q (10^{25} molecules s^{-1}) CN	C_3	CH	C_2	NH_2	$Af\rho$ (cm^{-1})	Q(OH)/Q(CN)[a]	$Q(H_2O)$ (10^{25} molecules s^{-1})[b]	GDR[c]
19850912	2.59	5.8 ± 2.0	...	...	...	...	1215 ± 304	316	1400	1.1 ± 0.2
19850914	2.56	9.2 ± 3.2	...	...	...	...	1257 ± 314	316	2100	1.2 ± 0.2
19850915	2.55	3.3 ± 1.2	...	...	...	...	597 ± 149	316	800	1.1 ± 0.2
19851211	1.33	20.6 ± 7.3	1.3 ± 0.5	55 ± 20	21.0 ± 4.3	12.4 ± 4.3	475 ± 119	354	5200	2.0 ± 0.2
19851213	1.30	28.7 ± 10.1	1.4 ± 0.5	47 ± 16	35.0 ± 12.3	8.4 ± 2.9	313 ± 78	354	7200	2.4 ± 0.2
19851214	1.28	30.8 ± 10.7	2.0 ± 0.7	...	40.4 ± 14.2	16.6 ± 5.8	1050 ± 263	354	7700	1.9 ± 0.2
19860110	0.87	110 ± 39	7.2 ± 2.5	2500 ± 875	144 ± 51	45 ± 16	6856 ± 1714	158	13000	1.3 ± 0.2
19860112	0.84	133 ± 47	5.0 ± 1.8	3100 ± 1085	204 ± 71	49 ± 17	5353 ± 1338	158	16000	1.5 ± 0.2
19860513	1.81	34 ± 12	3.0 ± 1.0	...	37.1 ± 13.0	27.9 ± 9.8	3095 ± 774	316	7700	1.4 ± 0.2
19860514	1.82	15.9 ± 5.6	1.8 ± 0.6	...	17.0 ± 5.9	...	1375 ± 344	316	3700	1.4 ± 0.2
19860608	2.17	44 ± 15	2.3 ± 0.7	...	15.8 ± 5.6	...	12006 ± 3002	200	6500	0.7 ± 0.2
19860610	2.2	34 ± 12	1.6 ± 0.6	...	22.8 ± 8.0	...	1790 ± 448	200	4900	1.4 ± 0.2

[a] From D. Schleicher 1993, personal communication.
[b] Derived quantity, see text.
[c] GDR = log [$Q(H_2O)/Af\rho$] − 24.

© American Astronomical Society • Provided by the NASA Astrophysics Data System

1994ApJ...433..886W

ized to the nucleus and was not visible in the two additional spectra obtained on June 8 at ~60,000 km offsets on the sunward and tailward sides of the nucleus. It is also possible that the increased dust production and relatively constant gas production on June 8 is due to a delay between the appearance of dust in a coma and the appearance of radicals which are typically produced hours to days after parent molecules are released from the nucleus. Thus, it is possible that the difference in GDRs on June 8 and 10 are due to the phase lags between dust and gaseous species.

Data sets obtained from the International Halley Watch CD-ROM archive were consulted to see if the outburst was observed in other data that night. Photometric observations with aperture sizes of 50″–80″ were obtained on June 8 on Mauna Kea which show a factor of 2 increase over June 10 observations in dust and C_3 production, while C_2 and CN show an increase of less than ~30% (Tholen 1992). Given the much larger aperture sizes of the photometric observations (our spectra were obtained with an aperture size of ~6″), the photometry is in good agreement with our observations and suggests that we were catching the beginning of an outburst. Comparison with light-curve data of comet Halley indicate that the outburst may be connected with an already identified active region on the comet which may be experiencing a seasonal effect (Schleicher 1993, private communication). We also note that the differences in GDRs could be due purely to the phase lags between dust and gaseous species. Thus, the existence of separate reservoirs is a possible interpretation of the data, but not the only one.

Therefore, we conclude that, while isolated outbursts may have resulted in notable changes in the GDR in comet Halley on timescales of weeks or days, there was no systematic dependence of the GDR on heliocentric distance between −2.6 and +2.2 AU. These data are then consistent with a nucleus that is largely homogeneous in dust and gas composition but which may also have independent reservoirs of gas and dust.

3.3. *Pre- versus Postperihelion Abundances of Gas and Dust*

As has been noted by several authors, comet Halley was more productive in both gas and dust after closest approach (Weissman 1987; Houpis 1989; Schleicher et al. 1990). Our data confirm these previous observations. In Figure 4 are plotted the log of production rates for individual species versus the log of heliocentric distance of comet Halley. The relatively weak CH feature was not observed in postperihelion data, and significant limits could not be set to its production for these dates. A power-law relationship between the production rates and heliocentric distance [$Q(X) \sim r^n$] was assumed, and an index, n, was derived using a least-squares fit to the preperihelion data. The slopes derived from the least-squares fits are shown in the figure and are in good agreement with results published elsewhere for comet Halley (e.g., Green & Morris 1987; Rozenbush et al. 1989). As the figure shows, the observed postperihelion production rates of CN, C_3, C_2, and NH_2 are 2–5 times greater at $r \sim 2$ AU during the outbound journey than they probably were at the same distance preperihelion. The dust production also appears to be about a factor of 2 larger in postperihelion data. Thus, it appears that the production of both volatiles and dust in comet Halley was substantially higher postperihelion.

After closest approach to the Sun, some comets appear to produce more gas and dust, while others are brighter preperihelion. Although commonly observed in comets, the

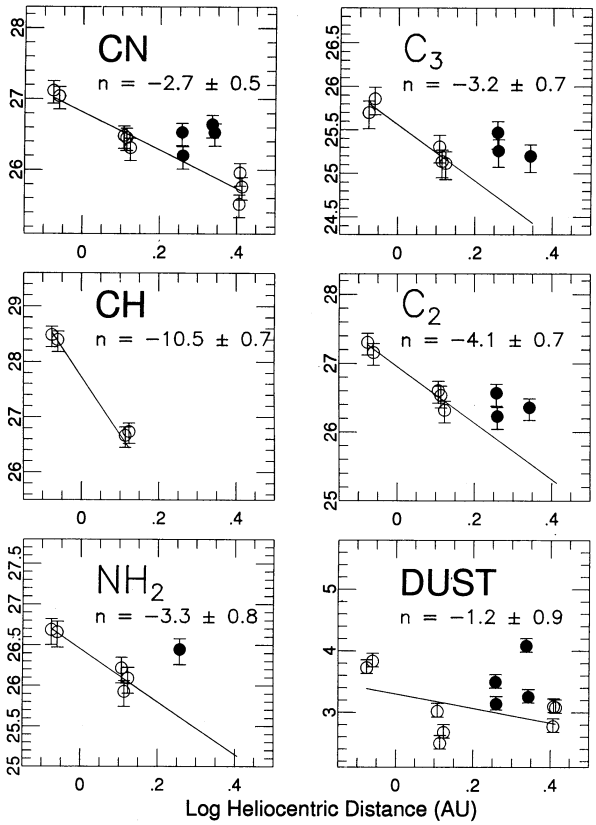

FIG. 4.—The y-axis represents the log of production rates for molecular species and log of $Af\rho$ for the dust continuum. Preperihelion points are given in open circles, while postperihelion points are shown with filled circles. The solid line is a least-squares fit to the preperihelion points. Note the increased production postperihelion.

reason for this asymmetrical behavior is not clear. The higher postperihelion abundances have been explained as due to a seasonal effect coupled with a complex rotational motion of the nucleus and the fact that the outgassing is limited to a few active spots for Halley (Weissman 1987). Alternatively, it has been suggested that thermal lag and mantle development with subsequent blowoff may play a significant role in the differing productions (Houpis 1989). More detailed modeling and observations of cometary gas and dust production rates over a large range of heliocentric distances are needed to better understand this behavior.

3.4. *Relative Abundances of Neutral Species*

It is often useful to compare the relative production rates of different molecules. Since CN is the most dominant feature in any optical cometary spectrum, and because CN is considered to be a good indicator of the overall gas production, other molecules are usually compared to it. In Figure 5 are plotted the log of $Q(C_3)$, $Q(C_2)$, $Q(NH_2)$, and $Af\rho$ versus log [Q(CN)]. Overall, there is an increase in each molecule's production rate as Q(CN) increases, while the correlation of dust abundance with Q(CN) appears weaker. Although very few points are available, no difference is seen in the postperihelion ratios compared with those obtained preperihelion, except perhaps for the dust. A least-squares fit was performed, assuming $Q(X) \sim [Q(CN)]^n$, to the preperihelion data, and the relationships between the production rates are shown in the panels of the figure. Within the uncertainties of our data, the production

© American Astronomical Society • Provided by the NASA Astrophysics Data System

1994ApJ...433..886W

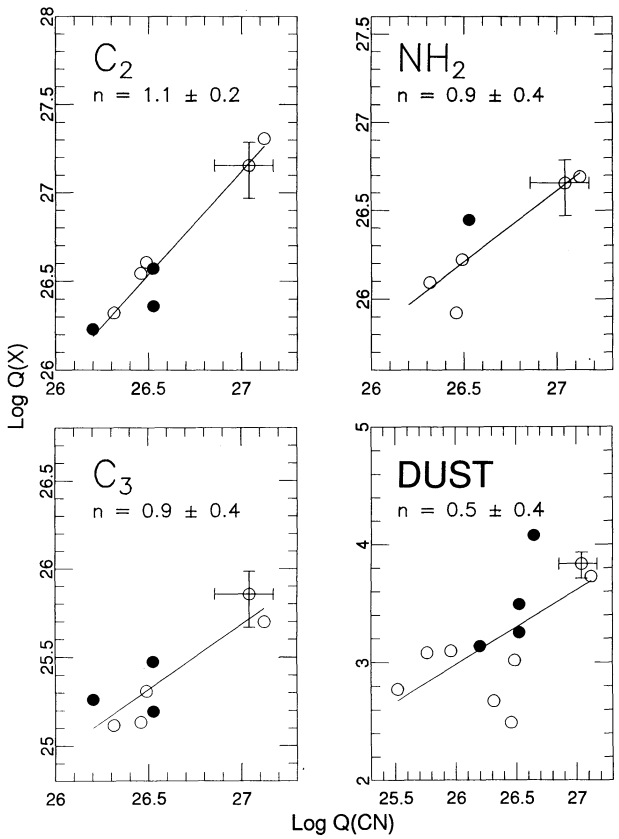

FIG. 5.—Log of production rate of the molecules C_2, NH_2, C_3, and CH vs. log of Q(CN). Preperihelion points are given in open circles, while postperihelion points are shown with filled circles. Solid lines represent least-squares fits to the data. The slope of the line, m, is given for each species.

rates of C_2, C_3, and NH_3 all appear to be entrained to that of CN. Although not shown in the figure, the slope of Q(CH) versus Q(CN) was 2.42 ± 0.31, which is not consistent with a direct relationship to CN. However, only four points were available for Q(CH), so the fit should be interpreted with caution. The slopes presented here are in good agreement with results derived recently from a large data set of comets by Cochran et al. (1992).

3.5. *The Spectral Continuum of Comet Halley*

The continuum spectrum of comets is largely produced by the scattering of solar radiation by grains in the coma. Comparison of the cometary continuum with the solar continuum, therefore, has the potential to provide information about the nature of the dust particles. Cometary spectra are usually observed to be redder than the sun (e.g., Gebel 1970; Cochran, Barker, & Cochran 1980; Remillard & Jewitt 1985), with reflectivity gradients that are consistent with grain sizes on the order of a few microns or less (e.g., Jewitt & Meech 1986), although some comets have been observed with blue continua (i.e., A'Hearn et al. 1979).

A reflectance spectrum was produced from our data by dividing an individual cometary spectrum by the spectrum of the solar analog star Van Bueren 64. The solar analog spectrum was found to agree with the overall shape of a theoretical solar spectrum to within 2% for the range of 4500–5500 Å. The amount of reddening was determined by measuring the reflectivity gradient, $dS/d\lambda$,

$$\frac{dS}{d\lambda} = \frac{S(5500\ \text{Å}) - S(4500\ \text{Å})}{S(\text{average})}, \qquad (3)$$

where S(average) is the average reflectivity over the 4500–5500 Å range. The reflectivity gradients are listed in Table 7 and are given in units of percent per 1000 Å.

TABLE 7

SPECTRAL REDDENING IN COMET HALLEY

UT Date	Offset (km)	P.A.	$dS/d\lambda$ (% per 1000 Å)	UT Date	Offset (km)	P.A.	$dS/d\lambda$ (% per 1000 Å)
1985 Sep 12	0	0°	−9.3 ± 5.0	1985 Dec 14	−8703	249	7.0 ± 5.0
1985 Sep 14	0	0	5.4 ± 4.0	1985 Dec 14	−17406	249	14.5 ± 5.0
1985 Sep 15	0	0	11.3 ± 7.0	1985 Dec 14	−23208	270	20.0 ± 6.0
1985 Dec 11	0	0	22.8 ± 8.0	1985 Dec 14	−31331	264	21.1 ± 6.0
1985 Dec 11	−10879	270	0.0 ± 5.0	1985 Dec 14	−34813	249	0.0 ± 5.0
1985 Dec 11	−21758	270	0.0 ± 5.0	1985 Dec 14	−40034	261	10.9 ± 5.0
1985 Dec 11	10879	90	0.0 ± 5.0	1985 Dec 14	23208	90	5.9 ± 5.0
1985 Dec 11	56026	67	17.3 ± 6.0	1986 Jan 10	0	0	9.3 ± 5.0
1985 Dec 11	75065	73	22.8 ± 8.0	1986 Jan 12	0	0	49.7 ± 8.0
1985 Dec 13	−10313	270	27.4 ± 8.0	1986 May 13	0	0	36.0 ± 7.0
1985 Dec 13	−12605	124	1.3 ± 4.0	1986 May 13	−29953	270	22.2 ± 7.0
1985 Dec 13	−12605	236	31.9 ± 8.0	1986 May 13	29953	90	26.5 ± 7.0
1985 Dec 13	−17189	143	7.1 ± 6.0	1986 May 14	0	0	6.1 ± 5.0
1985 Dec 13	−17189	217	26.5 ± 8.0	1986 May 14	−9653	270	0.0 ± 5.0
1985 Dec 13	10313	90	6.4 ± 5.0	1986 May 14	−21062	270	0.0 ± 5.0
1985 Dec 13	12605	56	12.8 ± 5.0	1986 May 14	−30715	270	0.0 ± 5.0
1985 Dec 13	12605	304	11.2 ± 5.0	1986 May 14	9653	90	0.0 ± 5.0
1985 Dec 13	17189	37	13.4 ± 5.0	1986 May 14	21062	90	0.0 ± 5.0
1985 Dec 13	17189	323	22.0 ± 5.0	1986 May 14	30715	90	0.0 ± 5.0
1985 Dec 13	22918	27	3.0 ± 5.0	1986 Jun 8	0	0	15.9 ± 5.0
1985 Dec 13	22918	333	23.4 ± 6.0	1986 Jun 8	−57419	270	−21.5 ± 7.0
1985 Dec 13	162147	69	15.3 ± 6.0	1986 Jun 8	57419	90	0.0 ± 5.0
1985 Dec 13	181627	71	0.0 ± 5.0	1986 Jun 10	0	0	30.9 ± 7.0
1985 Dec 14	0	0	14.3 ± 5.0				

© American Astronomical Society • Provided by the NASA Astrophysics Data System

1994ApJ...433..886W

As Table 7 shows, the spectra were typically "red" ($dS/d\lambda > 0$) for 70% of the spectra with an average value of ($dS/d\lambda$) ~ 17% per 1000 Å. Neutral spectra, or spectra with zero reddening, were distributed equally between the tailward and sunward sides of the coma. None of the spectra obtained at the nuclear position were neutral. The highest reddening, 50%, was observed toward the nucleus on 1986 January 12.

Only two "blue" spectra were observed, one on 1985 September 12 with ($dS/d\lambda$) = −9.3% per 1000 Å and another on 1986 June 8 with ($dS/d\lambda$) = −21% per 1000 Å. Interestingly, the extreme blue continuum on June 8 also coincides with a strong outburst of dust (described in § 3.2) and with the lowest GDR in our data set. Perhaps the dust released in the outburst was rich in smaller sized dust grains. The other blue spectrum was observed on 1985 September 12, where the second-lowest GDR in our data set was recorded. Thus, there may be a correlation between dust production and grain color as suggested by A'Hearn et al. (1979). There appear to be no relationships between the measured reflectivity gradients and GDRs of the other observations.

The authors would like to thank D. G. Schleicher and D. A. Pinnick for many helpful discussions and M. F. A'Hearn for constructive comments which significantly improved the paper. This research is supported in part by grant NAGW-2811, from the Planetary Astronomy Program of the National Aeronautics and Space Administration.

REFERENCES

A'Hearn, M. F. 1982, in Comets, ed. L. L. Wilkening (Tucson: Univ. of Arizona), 433
A'Hearn, M. F., Millis, R. L., & Birch, P. V. 1979, AJ, 84, 570
A'Hearn, M. F., Schleicher, D. G., Feldman, P. D., Millis, R. L., & Thompson, D. T. 1984, AJ, 89, 579
Allen, M. A., Bochner, B., van Dishoeck, E., Teger, S., & Wyckoff, S. 1989, BAAS, 21, 934
Byard, P. L., Foltz, C. B., Jenkner, H., & Peterson, B. M. 1981, PASP, 93, 147
Cochran, A. 1986, AJ, 90, 2609
Cochran, A. L., Barker, E. S., & Cochran, W. D. 1980, AJ, 85, 474
Cochran, A. L., Barker, E. S., Ramseyer, T. F., & Storrs, A. D. 1992, Icarus, 98, 151
Cochran, A. L., & Cochran, W. D. 1990, in Workshop on Observations of Recent Comets, ed. W. F. Huebner et al. (San Antonio: Southwest Research Institute), 22
Debi Prasad, C., Jockers, K., & Geyer, E. H. 1992, Icarus, 95, 211
Fink, U., Combi, M. R., & Disanti, M. A. 1991, ApJ, 383, 356
Gebel, W. L. 1970, ApJ, 161, 765
Green, D. W. E., & Morris, C. S. 1987, A&A, 187, 560
Hardorp, J. 1982, A&A, 105, 120
Haser, L. 1957, Bull. Acad. R. de Belgique, 43, 740
Houpis, H. L. F. 1989, in Comet Halley: Investigations, Results, Interpretations, Vol. 2, ed. John Mason (Sussex: Ellis Horwood), 173
Huebner, W. F., Keady, J. J., & Lyon, S. P. 1992, Ap&SS, 195, 294
Jewitt, D., & Meech, K. J. 1986, ApJ, 310, 937
Kurucz, R. L., et al. 1984, National Solar Observatory Atlas, No. 1 (Sunspot, NM: National Solar Observatory)
Lutz, B. L., & Wagner, R. M. 1986, ApJ, 308, 993
Lutz, B. L., Womack, M., & Wagner, R. M. 1993, ApJ, 407, 402
Meech, K. J., & Jewitt, D. C. 1987, A&A, 187, 585
Randall, C., et al. 1992, BAAS, 24, 3
Remillard, R. A., & Jewitt, D. C. 1985, Icarus, 64, 27
Rozenbush, V. K., Rspaev, F. K., Churyumov, K. I., Vid'machenko, A. P., & Gorodetskii, D. I. 1989, Soviet Astron. Lett., 15, 155
Schleicher, D. G. 1981, Ph.D. thesis, Univ. of Maryland
Schleicher, D. G., et al. 1990, AJ, 100, 896
———. 1993, in preparation
Tegler, S. C., & Wyckoff, S. 1989, ApJ, 343, 445
Tegler, S., Burke, L. F., Wyckoff, S., Womack, M., Fink, U., & DiSanti, M. 1992, ApJ, 384, 292
Tholen, D. 1992, Comet Halley Archive, CD-ROM Vol. USA_NASA_IHW_HAL_-0022, International Halley Watch (Greenbelt, MD: NASA/GSFC)
Wagner, M., & Lutz, B. 1992, Comet Halley Archive, CD-ROM Vol. USA_NASA_IHW_HAL_0019, 0020, 0021, 0022, International Halley Watch (Greenbelt, MD: NASA/GSFC)
Wagner, R. M., Lutz, B. L., & Wyckoff, S. 1987, ApJ, 322, 544
Weissman, P. R. 1987, A&A, 187, 873
Wyckoff, S., Tegler, S., Wehinger, P. A., Spinrad, H., & Belton, M. J. S. 1988, ApJ, 325, 927

© American Astronomical Society • Provided by the NASA Astrophysics Data System